

Charge trapping in polymer transistors probed by terahertz spectroscopy and scanning probe potentiometry

J. Lloyd-Hughes,^{1,*} T. Richards,² E. Castro-Camus,¹ H. Sirringhaus,² L.M. Herz,¹ and M.B. Johnston^{1,†}

¹*University of Oxford, Department of Physics, Clarendon Laboratory,
Parks Road, Oxford, OX1 3PU, United Kingdom*

²*University of Cambridge, Department of Physics, Cavendish Laboratory,
Madingley Road, Cambridge, CB3 0HE, United Kingdom*

(Dated: May 25, 2019)

We introduce a combination of terahertz time-domain spectroscopy and scanning probe potentiometry to investigate the dynamics of charge trapping in polymer field-effect transistors fabricated on a silicon gate. Upon application of a gate voltage to the transistors, a change in the transmission of terahertz radiation is found to occur. We demonstrate that this differential transmission signal arises from the hole accumulation layer on the polymer/insulator boundary inducing an electron-rich layer in the silicon gate that interacts effectively with the radiation. By implementing a model of the terahertz transmission through the device we extract the hole density in the transistor channel. On the prolonged application of a gate bias we observe an exponential decay in the differential transmission with a gate-voltage-dependent time constant of the order of 10^3 s, compatible with an increase in the density of trapped holes in the polymer channel. Taken in combination with scanning probe potentiometry measurements conducted on similar transistors, these results indicate that device degradation is largely a consequence of hole trapping, rather than changes in the mobility of free holes in the polymer.

PACS numbers:

The promise of printable, flexible electronic devices and displays has fuelled the development of the polymer field-effect transistor (pFET) over the past decade. However, the long-term performance of state-of-the-art pFETs is limited by degradation mechanisms that cause the threshold voltage to increase in magnitude.[1, 2, 3, 4, 5, 6] The principal effect is thought to be charge carrier trapping in either the organic semiconductor or at the semiconductor/insulator interface, which screens the applied gate voltage. In many structures the effect of contact resistance on device degradation needs to be considered, and can make the reliable extraction of the trapped-charge density solely from I-V characteristics a difficult task.[7] It is therefore desirable to use a non-contact technique, such as spectroscopy or potentiometry, to investigate charge trapping in pFETs. In this Letter, we report on a non-contact study of the degradation mechanisms in polymer FETs, performed using charge modulation spectroscopy in the terahertz frequency range. We demonstrate that this approach permits us to monitor the density of trapped holes in the accumulation layer, by coupling the low-mobility holes to higher-mobility electrons in the silicon gate. Correlation of these findings with scanning probe potentiometry measurements allows us to assess separately the contributions to transistor degradation arising from changes in the contact resistance, field-effect mobility and trapped-carrier density.

For our investigation, we have employed terahertz time-domain spectroscopy (THz-TDS, [8, 9]) to provide a broadband source of electromagnetic radiation in the range from 0.1 THz to > 10 THz ($1 \text{ THz} = 4.1 \text{ meV} = 300 \mu\text{m} = 33.4 \text{ cm}^{-1}$). In contrast to traditional spectroscopic techniques that record the intensity of light, THz-TDS measures the electric field amplitude of a pulse propagating in free space, allowing the complex conductivity of a thin-film to be determined directly. Terahertz radiation interacts strongly with charge carriers in a material, with a fractional transmission change $\Delta T/T$ (on injection or photoexcitation of charges) proportional to the conductivity of the thin film.[10] THz-TDS has been applied previously to photoexcited inorganic[11] and organic[12] semiconductors, and superconductors.[13]

A schematic diagram of the bottom-gate, bottom-contact polymer transistors fabricated for this study is shown in Figure 1. The semiconducting polymer poly[(9,9-dioctylfluorene-2,7-diyl)-co-(bithiophene)] (F8T2) was deposited through spin-casting from solution (in a layer 100 nm thick) onto an interdigitated gold array (channel length $40 \mu\text{m}$, finger width $50 \mu\text{m}$, total channel width 45 mm). The gate electrode comprised a lightly n-doped silicon wafer ($2.5 \times 10^{15} \text{ cm}^{-3}$) with a total thickness of 0.62 mm, and a 200 nm thick SiO_2 gate dielectric. The transistors exhibited p-type conduction upon application of a negative gate voltage and a source-drain bias.

We have used a terahertz time-domain spectrometer similar to the one described in Ref. 8 to measure the THz radiation transmitted through the transistor. A semi-insulating GaAs photoconductive switch biased with a

*Electronic address: james.lloyd-hughes@physics.ox.ac.uk

†Electronic address: m.johnston@physics.ox.ac.uk

20 kHz square wave at ± 150 V generated a single-cycle electric-field transient after photoexcitation by pulses from a Ti:Sapphire oscillator laser (10 fs, 75 MHz repetition rate, 400 mW beam power). Electro-optic sampling was used to detect the transmitted transient. To create charge-modulation effects, an a.c. square wave bias voltage V_g was applied to the gate, typically $V_g = 0 \leftrightarrow -30$ V at 40 Hz. For this experiment the source and drain contacts were connected to 0 V, and no source-drain current flowed. The modulation period (0.025 s) was chosen to be significantly longer than both the estimated channel formation time ($\sim 9 \mu\text{s}$) [14] and the RC time constant created by the contact resistance (~ 1 ms). Using a shorter modulation period did not alter the measured differential THz transmission. A lock-in amplifier was used to measure the change ΔT (resulting from the V_g modulation) in the THz electric field T transmitted through the transistors (Figure 1b). The THz beam and transistor were kept in a vacuum of 1 mbar to minimize THz absorption from atmospheric water vapor. In order to obtain good transmission (25%) through the device it was necessary to orient the transistor with the fingers of the interdigitated array at 90° to the plane of polarization of the incident THz electric field. However, in this geometry the interdigitated array diffracts the incident THz radiation at wavelengths close to the repeat period of the array ($\lambda = 90 \mu\text{m}$ in silicon, corresponding to 0.98 THz in vacuum). This results in a first diffraction minimum in $\Delta T/T$ near 1 THz (see Figure 1c, d) and further reductions at higher frequencies. We have therefore limited our data analysis (discussed below) to the unaffected free spectral range up to ~ 1 THz.

As an alternative experimental approach, the local surface potential on operating transistors was measured via non-contact potentiometry, using a scanning force microscope in Kelvin probe mode. Here, the voltage applied to the conducting tip is regulated by a feedback loop to minimize the electro-static force between tip and sample, with the resulting tip potential following the electrostatic potential in the accumulation layer. A detailed description of the experimental set-up and the methods employed for data analysis and processing can be found in Ref. [15].

Figures 1b and c display the measured change in THz electric field ΔT under the application of a bias $V_g = 0 \leftrightarrow -30$ V, which is approximately $250\times$ smaller than the size of the electric field T transmitted through the transistor. No transmission changes were observed after the F8T2 layer was chemically removed, or for devices fabricated without the polymer layer. Figure 1d shows that on the application of a gate bias the transistor transmits less THz radiation (negative $\Delta T/T$), indicating the creation of a partially reflective layer through changes in the charge carrier density. A negative V_g induces both a hole accumulation layer on the polymer/insulator boundary, and an electron accumulation layer of equal surface carrier density on the insulator/gate boundary (Figure 1a). The observed transmission change of THz radiation

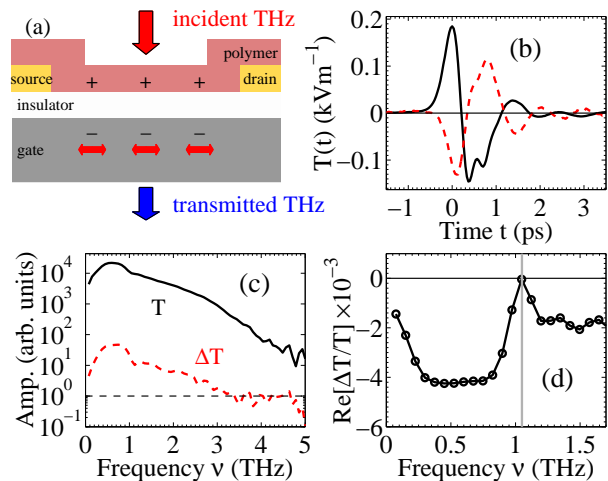


FIG. 1: (Color online) a) Schematic diagram of the transistor sample geometry for THz-TDS. Application of a negative gate voltage gives rise to holes in the accumulation layer in the polymer and highly-mobile electrons in the silicon gate. b) Measured THz electric field $T(t)$ after transmission through transistor (solid line) and change in transmitted THz electric field $\Delta T(t)$ (dashed line, multiplied by $\times 100$) upon application of a gate voltage $V_g = 0 \leftrightarrow -30$ V. Both are given as a function of electro-optic sampling delay time t . c) Amplitude spectra of the transmitted THz radiation $T(\nu)$, and change in transmitted amplitude $\Delta T(\nu) = T(V_g = -30 \text{ V}) - T(V_g = 0 \text{ V})$ obtained from the time-domain data in b) through Fourier transformation. d) Change in transmission $\Delta T/T$ as a function of frequency. The artefact close to 1 THz is a result of diffraction from the interdigitated array formed by the electrodes, as explained in the text.

with applied gate bias arises primarily from the electrons in the silicon, as the mobility of holes in the accumulation layer ($\mu = 7 \times 10^{-3} \text{ cm}^2 \text{ V}^{-1} \text{ s}^{-1}$, estimated from the current in the saturation regime) is more than five orders of magnitude lower than the electron mobility in the silicon gate ($\sim 1400 \text{ cm}^2 \text{ V}^{-1} \text{ s}^{-1}$). This interpretation is confirmed by the lack of a transmission change found for an all-polymer transistor (on a quartz substrate) within the experimental noise floor limit of $\Delta T/T < 1 \times 10^{-5}$. For silicon-gate polymer transistors the electron layer in the gate therefore acts as an indirect, but sensitive probe of the hole density in the polymer, by coupling it to higher mobility electrons in the silicon.

$\Delta T/T$ increases linearly with the applied gate voltage (Figure 2a), in accordance with an increase of charge density in the channel. We have modelled these data using standard thin-film transmission coefficients. The accumulation layer in the silicon gate was assumed to have a constant electron concentration N_e over a thickness δ_e at each gate voltage. The parameters used were in good accord with those obtained from an analytical solution of Poisson's equation at the SiO_2/Si boundary. The Drude-Lorentz model [16] was used to calculate the dielectric function of the electron layer, with scattering rate $\Gamma = 1.5 \times 10^{12} \text{ s}^{-1}$.

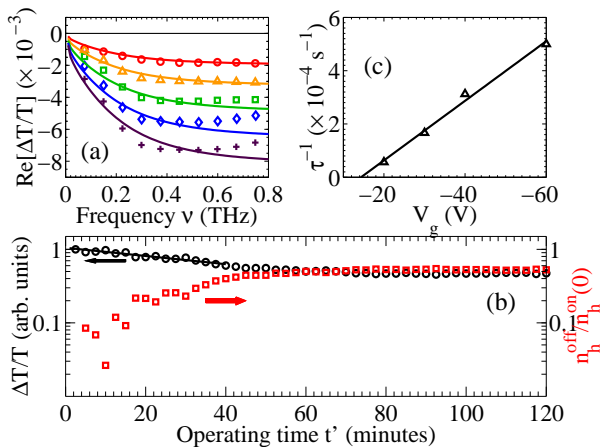


FIG. 2: (Color online) a) Measured differential transmission signal $\Delta T/T$ for a range of gate voltage modulations $0 \leftrightarrow V_g$ with $V_g = -10$ V (circles), -20 V (triangles), -30 V (squares), -40 V (diamonds), and -50 V (crosses). The solid lines are fits to the data based on a Drude-Lorentz thin-film model as described in the text, with $\Delta T/T \propto V_g \propto n_h$. b) When $V_g = 0 \leftrightarrow -30$ V is applied for times t' (half the measurement time, owing to the 50% V_g duty cycle) the differential transmission (circles) decays initially exponentially (straight line). The time constant $\tau = 7.1 \pm 2.4 \times 10^3$ s of this decay was determined by averaging fits for three nominally identical transistors, over the first 40 minutes. The trapped charge density remaining in the channel during the off period, $n_h^{\text{off}}(t')/n_h^{\text{on}}(0)$ (squares, extracted from the modelled fits to $\Delta T/T$, with charge density $n_h^{\text{on}}(0) = 3.2 \times 10^{12} \text{ cm}^{-3}$ when on) saturates at large t' . c) Hole trapping rate $1/\tau$ obtained from exponential fits to $\Delta T/T$ during application of $0 \leftrightarrow -V_g$ for 30 minutes.

Excellent agreement with the experimentally measured $\Delta T/T$ is obtained for an electron accumulation layer density of $N_e^{\text{off}} = 2.5 \times 10^{15} \text{ cm}^{-3}$ in the ‘off’ ($V_g = 0$ V) state and $N_e^{\text{on}} = 4.0 \times 10^{18} \text{ cm}^{-3}$ in the ‘on’ ($V_g = -30$ V) state when $\delta_e = 8$ nm, as shown in Figure 2a. The plasma frequency in the ‘off’ (‘on’) state is 0.2 THz (8.8 THz). Assuming that the sheet charge density in the polymer (n_h) is the same as that in the gate (n_e), the hole accumulation layer charge density for a pristine transistor in the ‘on’ state, N_h^{on} , can be calculated from $N_h^{\text{on}} = N_e^{\text{on}} \delta_e / \delta_h$, where δ_h and δ_e are the thickness of the hole and the electron accumulation layer, respectively. Taking $\delta_h = 1$ nm as a reasonable approximation we obtain $N_h^{\text{on}} = 3.2 \times 10^{19} \text{ cm}^{-3}$ at $V_g = 0 \leftrightarrow -30$ V, in good agreement with typical values found in the literature.[17] Using identical parameter values to those determined above for $V_g = -30$ V, but scaling n_e and δ_e linearly with gate voltage, results in model curves closely matching the measured $\Delta T/T$ over the entire range of applied V_g (see Figure 2a).

The sensitivity of our technique to the hole density in the transistor channel makes it an ideal tool to investigate the mechanisms governing degradation of these devices under prolonged application of a gate bias voltage. Measurements of $\Delta T/T$ as a function of biasing time (given

in Figure 2b) show an exponential decrease for approximately the first hour, after which the values gradually saturate. We attribute these changes to an increase in density of trapped holes at the polymer/insulator interface with time, resulting in a larger hole density n_h^{off} in the ‘off’ state (and therefore also an increased n_e^{off} , since trapped holes remain in the channel and contribute to the signal in the off state). Figure 2b displays n_h^{off} as a function of operating time, as extracted from the data using the model described above under the assumption that all other parameters are unaffected by degradation. The hole density for the ‘off’ state increases considerably within the first hour, but then saturates at a value of approximately half that of the initial value in the ‘on’ state, $n_h^{\text{on}}(0)$.

The exponential nature of the initial decay of the $\Delta T/T$ signal indicates that the hole trapping rate in the polymer is a linear function of the carrier density (i.e. $dn/dt = -n/\tau$) and therefore incompatible with the bipolaronic trapping mechanism ($dn/dt \propto n^2$) that has recently been proposed as a contributor to device degradation on timescales below 1 s.[3, 4] Figure 2c demonstrates that the initial trapping rate $1/\tau$, extracted from exponential fits to the initial decay, is proportional to the applied gate voltage. This linear rise in $1/\tau$ suggests that the trapping cross-section or the trap density (or both) increase with gate bias, as suggested recently by Salleo and Street.[4] We find that the decrease in $\Delta T/T$ is temporarily reversible under illumination, but only for photon energies above the polymer bandgap, confirming that the degradation mechanism is largely associated with changes in the polymer.[15, 18] Similar device recovery is also found after leaving the device with $V_g = 0$ V in the dark, as observed previously.[2] The modulation period used was too short to obtain significant carrier de-trapping during the ‘off’ state, and consequently we attribute the trapping dynamics to a combination of shallow and deep traps.

Finally, we compare the insights gained about polymer transistor degradation from THz-TDS techniques with those that may be obtained from more established techniques based on non-contact potentiometry.[19, 20] For this purpose, we have conducted scanning Kelvin-probe microscopy (SKPM) measurements, which can track the electrostatic potential in the accumulation layer with a high spatial resolution (< 100 nm). The F8T2 transistors investigated were similar to those examined using THz-TDS apart from a reduced channel length ($2 \mu\text{m}$), limited by the range of the SKPM tip. Figure 3 displays the resulting source-drain current I , contact resistance R and channel field-effect mobility $\mu_F = \mu_h n_h$ as a function of operating time of the F8T2 transistor. It can be clearly seen that the early non-exponential decay of I is caused by a rapid initial increase of the contact resistance with operating time.[21] The field-effect mobility, on the other hand, shows an initial exponential decay ($\tau = 1.2 \times 10^4$ s) comparable to that obtained from THz-TDS ($\tau = 7.1 \times 10^3$ s), before tending to saturate at longer

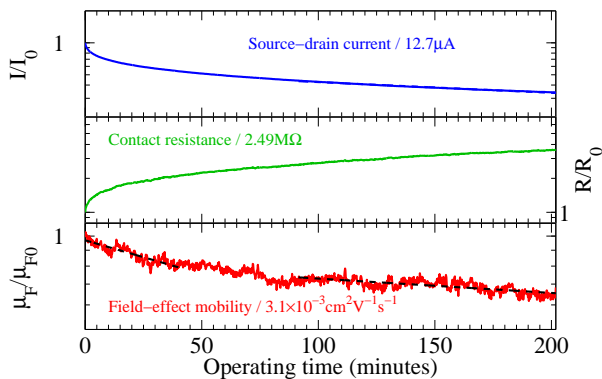


FIG. 3: (Color online) Source current (top), source contact resistance (middle) and field-effect mobility μ_F (bottom) of a $2\ \mu\text{m}$ channel length F8T2/300 nm SiO_2/Si pFET as a function of operating time, normalized to their initial values and shown on a semi-logarithmic plot. The curves were extracted from scanning Kelvin-probe microscopy measurements across the transistor channel. A constant gate voltage bias of $V_g = -40\ \text{V}$ was applied, to produce an initial sheet charge density $n_h = 2.9 \times 10^{12}\ \text{cm}^{-2}$ comparable to that in the THz experiments. The dotted lines are exponential fits to μ_F at early and late operating times, with time constants $\tau = 1.2 \times 10^4\ \text{s}$ and $\tau = 5.6 \times 10^4\ \text{s}$ respectively.

operating times. These results demonstrate the difficulty in extracting meaningful information about the dynamics of carrier trapping in pFETs from $I - V$ characteristics, which are significantly influenced by changes in contact resistance.[7] The observed decay of the field-effect mobility may be caused either by a decrease in hole mobility or hole density in the channel. The combined THz-TDS and SKPM measurements therefore suggest that the changes

in field-effect mobility with transistor operation time are dominated by a reduction in the density of mobile carriers, rather than a decrease in general mobility of all charges in the channel.

In conclusion, we have investigated the mechanisms for degradation of polymer-based FETs using a combination of THz spectroscopy and non-contact potentiometry. We find that the observed changes in THz transmission with application of a gate bias are caused by a layer of high-mobility electrons that forms in the silicon gate as mirror charges to the lower-mobility hole accumulation layer in the polymer. During the ‘on’ state of the transistor, the plasma frequency of the electron layer is shifted upwards in frequency, permitting highly sensitive, non-contact probes of the accumulated charge density through THz-TDS. Our measurements demonstrate an initial mono-exponential decrease of the THz differential transmission signal with biasing time, in agreement with an increase of trapped charge density in the polymer present also during the ‘off’ state. Complementary SKPM measurements show that the contact resistance strongly influences the source-drain current at early device operation times ($<40\ \text{min}$). $I - V$ curves taken on their own therefore do not provide direct access to the charge-trapping dynamics in pFETs. By being sensitive only to electrons in the silicon gate, the THz-TDS measurements are not influenced by the hole mobility in the polymer. From the results of both THz-TDS and SKPM techniques we infer that an increase in trapped-charge density, rather than a decrease in single-carrier mobility, is responsible for the decline in field-effect mobility with operation time.

The authors would like to acknowledge support by the EPSRC for this work.

-
- [1] H. Sirringhaus, *Adv. Mat.* **17**, 2411 (2005).
 - [2] A. Salleo and R. A. Street, *J. Appl. Phys.* **94**, 471 (2003).
 - [3] R. A. Street, A. Salleo, and M. L. Chabinye, *Phys. Rev. B* **68**, 085316 (2003).
 - [4] A. Salleo and R. A. Street, *Phys. Rev. B* **70**, 235324 (2004).
 - [5] A. Salleo, F. Endicott, and R. A. Street, *Appl. Phys. Lett.* **86**, 263505 (2005).
 - [6] K. P. Pernstich, S. Haas, D. Oberhoff, C. Goldmann, D. J. Gundlach, B. Batlogg, A. N. Rashid, and G. Schitter, *J. Appl. Phys.* **96**, 6431 (2004).
 - [7] L. Burgi, T. J. Richards, R. H. Friend, and H. Sirringhaus, *J. Appl. Phys.* **94**, 6129 (2003).
 - [8] M. B. Johnston, L. M. Herz, A. L. T. Khan, A. Köhler, A. G. Davies, and E. H. Linfield, *Chem. Phys. Lett.* **377**, 256 (2003).
 - [9] D. Grischkowsky, S. Keiding, M. van Exter, and C. Fattinger, *J. Opt. Soc. Am. B* **7**, 2006 (1990).
 - [10] K. P. H. Lui and F. A. Hegmann, *Appl. Phys. Lett.* **78**, 3478 (2001).
 - [11] R. Huber, F. Tauser, A. Brodschelm, M. Bichler, G. Abstreiter, and A. Leitenstorfer, *Nature* **414**, 286 (2001).
 - [12] E. Hendry, J. Schins, L. P. Candeias, L. D. A. Siebbeles, and M. Bonn, *Phys. Rev. Lett.* **92**, 196601 (2004).
 - [13] M. C. Nuss, K. W. Goossen, J. P. Gordon, P. M. Mankiewich, M. L. O’Malley, and M. Bhushan, *J. Appl. Phys.* **70**, 2238 (1991).
 - [14] L. Burgi, R. H. Friend, and H. Sirringhaus, *Appl. Phys. Lett.* **82**, 1482 (2003).
 - [15] L. Burgi, T. Richards, M. Chiesa, R. H. Friend, and H. Sirringhaus, *Synth. Met.* **146**, 297 (2004).
 - [16] C. Kittel, *Introduction to Solid State Physics* (Wiley, 1996), chap. 10, pp. 270–273.
 - [17] C. Tanase, E. J. Meijer, P. W. M. Blom, and D. M. de Leeuw, *Org. El.* **4**, 33 (2003).
 - [18] J. Lloyd-Hughes, T. Richards, E. Castro-Camus, H. Sirringhaus, L. M. Herz, and M. B. Johnston, Unpublished (2006).
 - [19] L. Burgi, H. Sirringhaus, and R. H. Friend, *Appl. Phys. Lett.* **80**, 2913 (2002).
 - [20] V. Palermo, M. Palma, and P. Samori, *Adv. Mater.* **18**, 145 (2006).
 - [21] This will be discussed in detail elsewhere.